Pure & Appl. Chem., Vol. 56, No. 10, pp 1379-1390, 1984.
Printed in Great Britain.

0033-4545/84 $3.00+0.00
Pergamon Press Ltd.

COOPERATIVE MOTION AND SELF-DIFFUSION IN DILUTE AND SEMIDILUTE POLY-VINYLPYRROLIDONE SOLUTIONS

Walther Burchard and Michael Eisele

Institut für makromolekulare Chemie, Universität Freiburg, Stefan-Maier-Straße 31, Federal Republic of Germany

Abstract - After a general introduction to the technique of dynamic light scattering, measurements from aqueous polyvinyl-pyrrolidone solutions in a concentration range up to 6 c* are reported, where c* is the coil overlapping concentration. In dilute solutions only one diffusion process was observed. Above c*, however, the time correlation function decays in two steps, and the slow mode gains quickly influence with increasing concentration. The fast and slow diffusion coefficients follow power laws of the type $D \sim (c/c^*)^{exp}$ with exponents of 0.60 and -1.50 for the fast and the slow modes. These exponents are lower in value than 0.75 and -1.75 as was predicted by de Gennes for semidilute solutions on the basis of scaling concepts. The mean square radius of gyration was found to increase sharply above c* in contrast to the prediction for reptating chains, where the radius should slightly decrease. The experimental findings are interpreted being caused by the motion of loosely entangled clusters.

INTRODUCTION

This contribution deals with an experimental study of polyvinyl-pyrrolidone solutions in a concentration range from dilute solutions up to 6 times the overlapping concentration c*. The homodyne dynamic light scattering technique has been applied in combination with conventional or static light scattering, and it is this combination of the two light scattering (LS) techniques which gives us, as we believe, new insight into the structure of the semidilute solution.

Since this is the first paper in a series of other contributions on the application of dynamic LS it will be useful to give here a short introduction to this method and to point out some new possibilities of characterizing polymer systems. In a second part we will review in brief the present understanding of a semidilute solution which has largely been formed by a picture drawn by de Gennes. Finally in the last part we will present our recent results obtained with polyvinyl-pyrrolidone (PVP), which may lead to some refinement of the de Gennes picture.

LINE WIDTH AND TIME CORRELATION FUNCTION

The basic idea of dynamic light scattering comes from the electromagnetic theory of moving transmitting sources according to which a shift to higher or lower frequencies occurs if the source moves towards the detector or in opposite direction, respectively. The magnitude of this shift depends on the ratio v/c_o of the source velocity to the speed of light propagation c_o. For randomly moving sources these Doppler shifts will result in a line width broadening of the Rayleigh line, and this broadening is proportional to the translational diffusion coefficient D (Ref. 1). For gases the line width broadening is remarkable and is easily recorded by common spectroscopy (Ref. 2,3). The velocities of molecules in solution are, however, fairly low and give rise to an only tiny line width broadening. Still the effect became detectable by Fabry-Perot spectroscopy of the scattered line when lasers came up as powerful, highly monochromatic light sources, and first pioneering dynamic LS measurements were carried out by this technique (Ref. 4,5). Unfortunately, the translational motion is slowed down appreciably with increasing chain length, and this fact confined direct spectroscopy to the

range of oligomers.

In the early 1930th Wiener (Ref. 6) and Khintchine (Ref. 7) discovered independently that there always exists a well behaved function $S(t)$ in the time domain which is adjoined to the power spectrum $S(\omega)$ in the frequency domain, where $S(\omega)$ and $S(t)$ are pairs of Fourier transforms, i.e.

$$S(\omega) = (2\pi)^{-1} \int_{-\infty}^{+\infty} S(t)\, e^{i(\omega t)}\, dt$$

$$S(t) = \int_{-\infty}^{+\infty} S(\omega)\, e^{-i(\omega t)}\, d\omega$$

The value of this Wiener-Khintchine theorem becomes evident if a constant value of ωt is considered. Now, if ω is small, and too small as to be detectable by spectroscopy, there exists associated to this line width broadening a large time interval which is often large enough to allow computations by special fast computers. Figure 1 shows the corresponding regions in the frequency and the time domains.

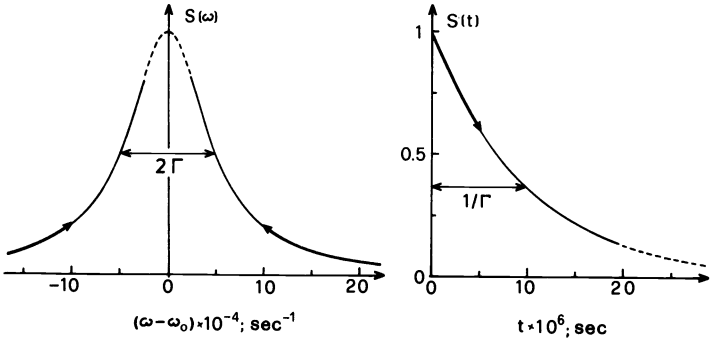

Fig. 1. Line shape of a power spectrum (left) and the corresponding time correlation function S(t). Corresponding domains are indicated by the same type of lines.

The idea of determing S(t) in the time domain rather than $S(\omega)$ in the frequency domain was taken up by the British group around E.R. Pike (Ref. 8) and eventually resulted in the construction of autocorrelators, by which the basic framework of modern dynamic LS measurements became completed. Nowadays we can state that there exists essentially no upper limit in the molecular weight for the application of dynamic LS; but there is still a gap at the short time end of about 10^{-7} to 10^{-9} seconds where motions are too fast for the construction of the autocorrelation function S(t) but on the other hand still too slow for a sufficient line width broadening. This region is characteristic for internal motions in flexible macromolecules.

SCATTERING INTENSITY TIME CORRELATION FUNCTION

In conventional LS a large scattering volume and long time of recording is chosen. Under such circumstances all fluctuations resulting from the motion of the molecules are averaged out. Hence only static properties are measured. In dynamic LS the scattering volume is made small (typically ≈ 0.008 mm^3) and the time of recording short (10^{-6} seconds in order) and now the scattering intensity shows strong fluctuations as shown schematically in Fig. 2

These fluctuations do not result from a variation of the number of molecules in the scattering volume but are caused by incidental clustering of molecules, giving rise to a strong scattering intensity, followed by a dissociation whereupon only little light is scattered.

Thus these fluctuations contain information on the mobility of the macromolecules which can be extracted as follows. Let A_i be the number of photons

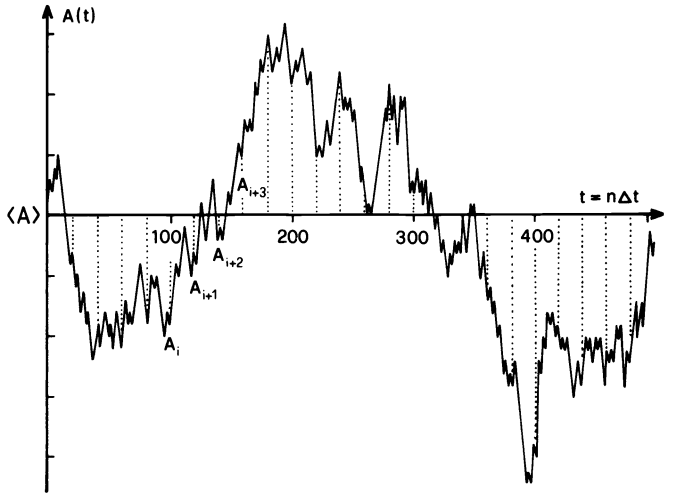

1 st channel: $\langle A_0 A_1 \rangle = \sum_i^N (A_i\, A_{i+1})$

2 nd channel: $\langle A_0 A_2 \rangle = \sum_i (A_i\, A_{i+2})$

n th channel: $\langle A_0 A_n \rangle = \sum_i (A_i\, A_{i+n})$

$N = 10^5$

$\langle i(0)i(t) \rangle = \langle A_0 A_n \rangle \equiv G_2(t)$

Fig. 2. Intensity fluctuations around the mean. A_i denotes the number of photons arriving at the detector in a time interval Δt.

arriving at the detector in the time interval Δt. With the help of a fast computer the number of photons from two successive time intervals are multiplied, and the product is stored in a first channel of the correlator. This procedure is repeated about 100 000 times and stored in channel 1. In channel 2 the products of photon numbers A_i and A_{i+2} are stored etc., and eventually in the last channel n the products of A_i and A_{i+n} are collected. The result of this manipulation is shown in Fig. 3a. The exponentially decaying function is called the time correlation function (TCF) of the scattering intensity. This name is easily understood if we recall that the time interval for the recording of photons was chosen very small such that most of the molecules have not yet collided with others. They thus have a good memory of the direction and magnitude of their velocities just one time interval before. However, after a longer delay time the molecules will have suffered many collisions and will have lost all memory of their initial velocity. Hence the curve in Fig. 3 describes the decay from a highly correlated to a fully uncorrelated motion. One notices from Fig. 2 that fluctuations occur around an average which is the scattering intensity that is recorded in static LS.

PROPERTIES OF THE TIME CORRELATION FUNCTION

The recorded TCF of the scattered light is in general not simply related to the motion of the molecules. In most cases, however, the following approximation holds to a sufficient accuracy (Ref. 9).

$$\langle i(0)i(t) \rangle = A + |g_1^2(t)| = G_2(t) \qquad (1)$$

where

$$g_1(t) = \frac{\langle |E^*(0)E(t)| \rangle}{\langle E^*(0)E(0) \rangle} = \frac{S(t,q)}{S(q)} \qquad (2)$$

with $$q = (4\pi/\lambda)\, \sin\theta/2 \qquad (3)$$

$g_1(t)$ is the normalized TCF of the scattered electric field. The denominator in eq.(2) will be recognized as the static structure factor and S(t,q) is the dynamic structure factor.

For monodisperse particles small in diameter compared to the wavelength of the light and also for hard monodisperse spheres of any size $g_1(t)$ is easily calculated and is a single exponential (Ref.9).

$$g_1(t) = \exp(-\Gamma t) = \exp(-Dq^2 t) \qquad (4)$$

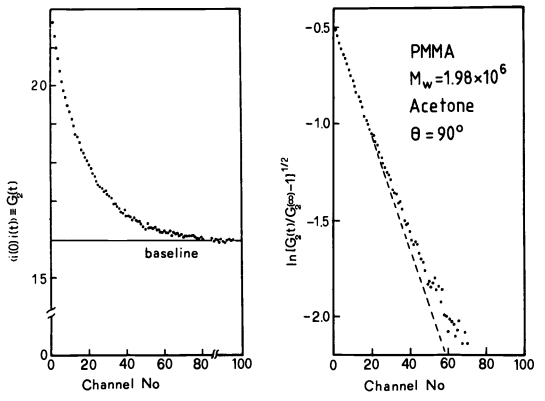

(a) (b)

Fig. 3. Scattering intensity TCF (a) and corresponding field TCF (b) for a PMMA sample of narrow molecular weight distribution.

In most cases, however, the decay of $g_1(t)$ is more complex, and the TCF shows a more slowly decaying tail. Such tail can be seen already with the monodisperse polymethyl-methacrylate sample shown in Fig. 3b. This behavior may result either from polydispersity or from internal modes of motion. Both effects may be demonstrated with two highly simplified examples.

POLYDISPERSITY

Let us assume that our system contains only two species of molecules of different sizes. Then the TCF consists of two exponentials

$$g_1(t) = a(q) \exp(-D_1(q^2t)) + b(q) \exp(-D_2(q^2t)) \qquad (5)$$

where D_1 and D_2 are the diffusion coefficients of the two particles. The coefficients $a(q)$ and $b(q)$ are the corresponding amplitudes which in general depend on the scattering angle. They are related to the particle scattering factors of the two particles. Sometimes, if $D_1 \ll D_2$, it is advisible to plot $g_1(t)$ against log t since $g_1(t)$ is spread out in such cases over several decades in time. In the present case it is useful to choose q^2t as a variable, because for measurements at different angles the decay of the two processes should occur at the same values of q^2t. The curves will in general not coincide, since the amplitudes may, as pointed out already, change with q. An experimental example will be discussed in greater detail later in this paper.

INTERNAL MODES OF MOTION

A flexible or soft particle will perform a number of internal modes of motion. These motions result in local segment density fluctuations and give additional contributions to the TCF with a characteristic time which corresponds to the relaxation time superimposed to the diffusive translational motion. Again, we may consider here the simplest case where only the longest internal motion contributes to the TCF with a sufficient amplitude. Then $g_1(t)$ is given by (Ref. 1,10)

$$g_1(t) = a(q) \exp(-D(q^2t)) + b(q) \exp-(D+1/\tau_1 q^2)(q^2t) \qquad (6)$$

where τ_1 is the relaxation time of the internal motion which cannot depend on the scattering angle. Therefore, in a plot of $g_1(t)$ against q^2t only the slowest and diffusive process will occur at the same values of the abscissa if different angles are chosen, while the second process will show a shift to smaller values of q^2t. An experimental example will be given below.

FIRST CUMULANT

Deviations from a single exponential are frequently observed and are the

rule rather than an exception. Separation of the TCF into the contributions from the various relaxation processes is in most cases difficult and sometimes not possible at all. In such cases ,however, the initial part of the TCF can be analysed. As it was first shown by Koppel (Ref. 11) and Pusey (Ref. 12) it is always possible to apply a cumulant expansion, i.e.

$$\ln g_1(t) = -\Gamma_1 t + (\Gamma_2/2!)t^2 - (\Gamma_3/3!)t^3 + \ldots \quad (7)$$

where Γ_1, Γ_2, etc. are the first , second etc. cumulants. The first cumulant is of particular interest since it can be calculated by equilibrium statistical mechanics (Ref. 13) and can be measured with high accuracy. One result of these calculations is the first term in a series expansion of the cumulant in terms of q^2 (Ref. 14)

$$\Gamma = D_c q^2(1 + C\langle S^2\rangle q^2 - \ldots) \quad (8)$$

where we have dropped the index 1. In this equation D_c is the translational diffusion coefficient at a concentration c, $\langle S^2\rangle$ the mean square radius of gyration and C a dimensionless coefficient which is characteristic for the architecture of the molecules. For instance, hard spheres are characterized by C = 0; flexible monodisperse linear chains have a value of C = 0.1773 Ref. 14). Branching causes a decrease in C and polydispersity an increase.

Extrapolation of $\Gamma/q^2 = D_{app}(q)$ against $q^2 = 0$ yields the diffusion coefficient at the finite concentration c. Often a linear concentration dependence is observed

$$D_c = D_z(1 + k_d c) \quad (9)$$

where D_z is the z-average zero concentration diffusion coefficient and k_d can be positive or negative depending on the magnitude of A_2M_w, where A_2 is the second virial coefficient and M_w the weight average molecular weight. Applying the Stokes-Einstein relationship to D_z we can define a hydrodynamically effective radius R_h

$$D_z = (kT/6\pi\eta_o)\langle 1/R_h\rangle_z \quad (10)$$

and furthermore, together with the radius of gyration, a dimensionless parameter (Ref. 14)

$$\rho = \langle S^2\rangle_z^{1/2}\langle 1/R_h\rangle_z \quad (11)$$

Again this dimensionless ρ-parameter is sensitive to the structure of the molecules, i.e. branching, ring formation, chain stiffness etc.

COMBINATION WITH STATIC LIGHT SCATTERING

It is instructive to compare eq.(8) and (9) with Debye's relationship for the static LS from not too large molecules

$$Kc/R(q) = (1 + 1/3\langle S^2\rangle_z q^2)/M_{app} \quad (12)$$

with

$$1/M_{app} = (1/M_w)(1 + 2A_2M_w c + \ldots) \quad (13)$$

$D_{app}(q)$ and $Kc/R(q)$ show a similar $\langle S^2\rangle q^2$ dependence and D_c and $1/M_{app}$ a similar concentration dependence. Static LS measurements are commonly evaluated from Zimm plots where $Kc/R(q)$ is plotted against q^2+kc. A similar dynamic Zimm plot can now be constructed with D_{app} (Ref.15).

Figure 4 shows as an example the static and dynamic Zimm plots of LS measurements from a polystyrene sample of 2.8×10^6 in molecular weight (Ref.15). Both sets of data were measured in this case simultaneously with the same instrument. Hence from such combined static and dynamic LS measurements 6 quantities are obtained , which are listed in Table 1.

These quantities can be combined to give the two dimensionless parameters C and ρ, as already described, and another coefficient k_{fo} (Ref. 16-19)

$$k_{fo} = k_f(M_w/N_A V_h) \quad (14)$$

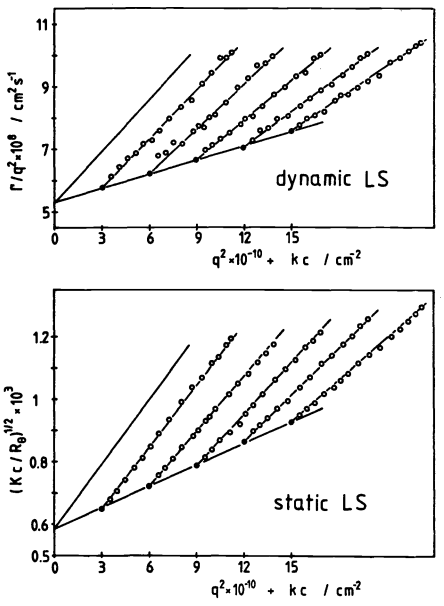

Fig. 4. Dynamic and static Zimm plots obtained with a polystyrene of $M_w = 2.8 \times 10^6$ in toluene at 20° C.

which is a measure for the interpenetration of two coils in a good solvent. In this equation k_f is the coefficient in a linear concentration dependence of the frictional coefficient

$$f_c = f(1 + k_f c + \ldots) \tag{15}$$

Table 1. List of quantities which can be obtained from dynamic and static Zimm plots shown in Fig.4

	inter-cept	slopes c=0	slopes q=0
static LS	M_w	$\langle S^2 \rangle_z$	A_2
dynamic LS	D_z	$C\langle S^2 \rangle_z$	k_D

and V_h is the hydrodynamic volume of the molecule which can be calculated from the hydrodynamic radius defined in eq.(10). The three coefficients k_D, k_f and A_2 are related to each other (Ref.19)

$$k_D + k_f = 2A_2M_w - v_2 \tag{16}$$

where v_2 is the partial specific volume of the polymer in solution.

In a theta solvent, where the coils can penetrate almost freely, Pyun and Fixman (Ref. 17) found in an estimation a value of $k_{f\Theta} = 2.23$, and in a good solvent they found $k_{f0} = 7.16$. These predictions agree satisfactorily with experiments from PMMA and PS in good and theta-solvents (Ref. 20,21).

SEMIDILUTE SOLUTIONS

So far only dilute solutions have been considered where the individual coils are well separated from each other and where the properties of individual particles can be studied. At concentration c* a different behavior may be expected. See Fig. 5.

In the picture of de Gennes (Ref.22) this behavior is governed by the correlation length ξ and the overlapping concentration c* which is used as a scaling parameter for the actual concentration. The correlation length descri-

bes the mesh size in a network and may be approximated by the chain length between points of entanglements. See Fig. 6.

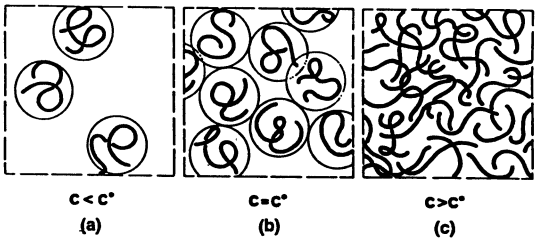

Fig. 5. Three typical stages of polymers in solution at different concentration. (From de Gennes Ref. 22).

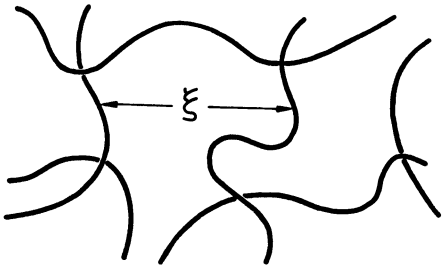

Fig. 6. Definition of the correlation length ξ .From de Gennes (Ref. 22).

De Gennes derived for good solvents on the basis of scaling arguments (Ref.22)

$$\xi = a\,(c/c^*)^{-0.75} \tag{17}$$

with **a** a not further defined length. In the dilute regime, i.e. c<c*, one has

$$\xi = \langle R^2 \rangle^{1/2} \tag{18}$$

where $\langle R^2 \rangle$ is the mean square end-to-end distance.

Because of the entanglements there is no longer a free motion of the molecules. De Gennes predicts two types of motion, i.e. a cooperative 'diffusion' of segments in the network and a self-diffusion of individual chains through the network.

The cooperative motion of a network consists actually of a series of normal modes. In such a weak gel most of these modes are very slow and cannot be detected by dynamic LS. The only mode which lies in the same time scale as the translational diffusion coefficients of freely moving individual molecules corresponds to an irregular motion of the center of mass of chains with a correlation length ξ, and this irregular motion has the appearence of a diffusion and is thus called a cooperative diffusion. Similar results have been obtained by Tanaka et al. (Ref. 23) with a theory of a continous elastic body. In the scaling theory by de Gennes the cooperative diffusion coefficient is given by

$$D_{coop} = kT/(6\pi\eta\xi) \cdot (c/c^*)^{0.75} \tag{19}$$

while in the theory of Tanaka et al. one has

$$D_{coop} = M/\rho f \tag{20}$$

with the longitudinal modulus $M = K + 4/3\mu$, the friction coefficient f and ρ the segment density (number of links per volume). For further details see Ref. 34.

Concerning the self-diffusion, de Gennes (Ref. 24) was led by the picture shown in Fig. 7. Apparently a chain surrounded by the obstacles of so many other chains has scarcely a chance for a motion transversally to its contour

length but it can move along its own contour length. This motion is slowed down remarkably with increasing chain length but also with creasing concentration. Again on the basis of scaling arguments de Gennes predicts the following chain length and concentration dependence (Ref.24).

$$D_{self} \sim N^{-2}(c/c^*)^{-1.75} \qquad (21)$$

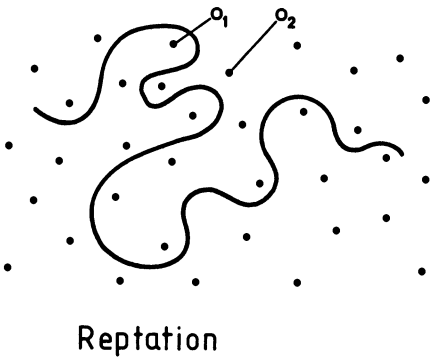

Fig. 7. Motions of a chain in an entangled system (Ref.22)

EXPERIMENTAL RESULTS WITH PVP SOLUTIONS

Fast and slow modes of motion have been recently observed by several authors in semidilute solutions of various polymers (Ref.25-30). Here we present now some new data obtained with aqueous and ethanolic solutions of PVP. Both solvents are thermodynamically good for this polymer. Measurements have been carried out in the range from 0.1c* to 5.9c*, where $c^* = 1/[\eta]$ was chosen. Figure 8 shows the TCF for five selected concentrations. Here $g_1(t)$ is plotted against log(t) which became necessary since the TCF extended over up to five decades in time. A single exponential has in this plot an S-shaped appearence similar to the curves for the two lowest concentrations in Fig. 8.

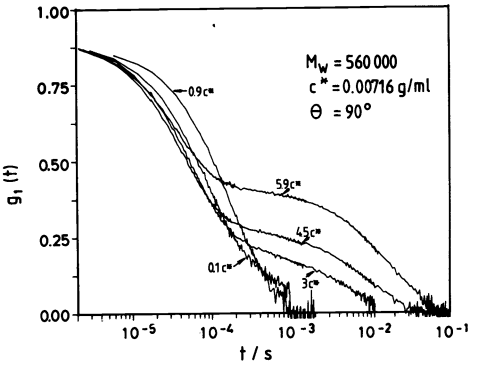

Fig. 8. TCF's for a PVP sample at 5 different concentrations

When c* is exceeded a second much slower process becomes noticeable. It gains quickly influence when the concentration is increased. The TCF is strongly angular dependent. However, if $g_1(t)$ is plotted against $\log(q^2t)$ the two processes occur at the same values of the abscissa. Consultations of eq. (5) makes it clear that both processes are diffusive (see Fig. 9).

Applying the CONTIN program by Provencher (Ref.35) we have been able to analyse the TCF's with respect to these two main relaxation times and their corresponding amplitudes. The analysis offers no difficulties when $c > c^*$ but becomes uncertain in the region of c below c* because of the low amplitude of the slow mode. The results of this analysis is shown in Fig. 10, where

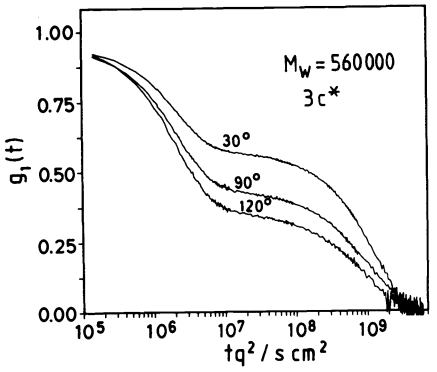

Fig. 9. TCF's of a PVP at $c = 3c^*$ and for various scattering angles, here plotted against tq^2.

both diffusion coefficients D_{fast} and D_{slow} are plotted as function of c/c* in a double logarithmic scale. The exponents of the fast and slow modes are with 0.6 and -1.50 both lower in value than predicted by de Gennes for an entangled system. Figure 10 contains two further diffusion coefficients which will be discussed later in this paper.

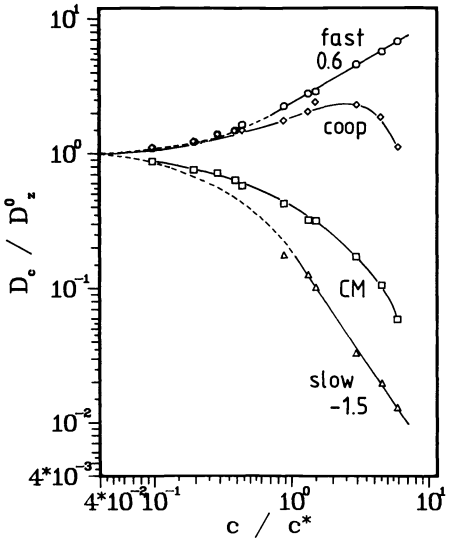

Fig. 10. Double logarithmic plot of the various diffusion coefficients, defined in the text, against c/c*. The numbers indicate the exponents.

At this point we may wonder of what origin the slow mode is. Do we really observe reptation or is it possibly something else? We could obtain some additional information from static LS which was recorded simultaneously with the dynamic LS data. Assuming validity of Debye's LS equation even for concentrations up to 5%

$$\frac{Kc}{R(q)} = \frac{1 + 1/3\langle S^2\rangle_c q^2}{M_w} + 2A_2c + \ldots = \tag{22}$$

$$= (1/M_w + 2A_2c + \ldots)(1 + 1/3\langle S^2\rangle_{app} q^2)$$

we can define an apparent mean square radius of gyration, which actually is a sort of correlation length, and which is influenced by thermodynamic interactions among chains. The direct influence of the virial coefficient can be eliminated since according to eq. (22) one has (Ref.31)

$$\langle S^2\rangle_c = \langle S^2\rangle_{app}(M_w / M_{app}) \tag{23}$$

where

$$1/M_{app} = 1/M_w + 2A_2c + 3A_3c^2 + \ldots = Kc/R(q)_{q=0} \quad (24)$$

Both $\langle S^2\rangle_{app}$ and $\langle S^2\rangle_c$ are plotted against c/c* in a double logarithmic scale in Fig. 11. Up to c = c*, $\langle S^2\rangle_{app}$ decreases and $\langle S^2\rangle_c$ remains essentially constant; beyond c*, however, the correlation lengths increase sharply by a factor 7. Such behavior does not correspond to a reptating individual chain which is generally assumed to remain in the randomly coiled form. The chains are swollen by the strong interaction with the good solvent, but the extent of swelling is predicted to decrease at higher concentrations due to shielding effects of the presence of the other chains according to a power law (Ref.33)

$$\langle S^2\rangle \sim (c/c^*)^{-0.25} \quad (25)$$

The contrary is observed.

We thus propose another explanation for the slow mode observed in the limited range of our measurements. It appears conceivable that transient clusters of loosely entangled chains are formed which can move only under heavy restrictions. Possibly the clusters do not move in toto, but motion may be realized by dissociation of individual chains from a cluster by followed

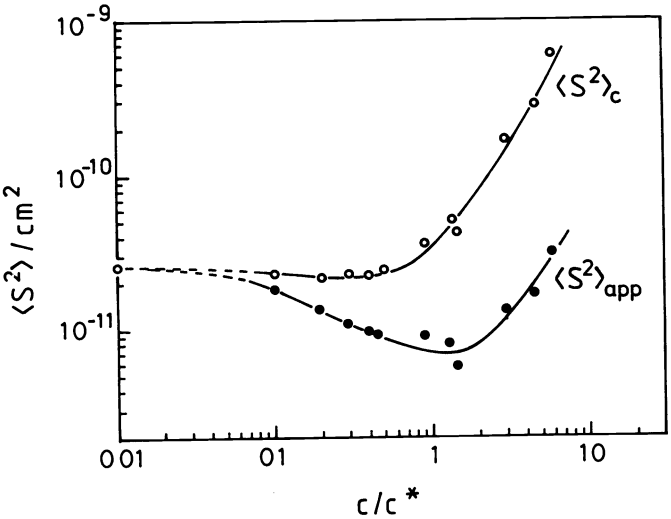

Fig. 11. Concentration dependence of the mean square radius of gyration (correlation length). For definition of $\langle S^2\rangle_c$ and $\langle S^2\rangle_{app}$ see eq. (23).

reptation and reassociation to another cluster. In other words, what is seen may be the result of a strong interaction of reptating chains with the matrix. This picture of clusters is supported by Fig. 12 where the amplitude w_{slow} of the slow mode is plotted against c/c* (w_{slow} has been determined for various scattering angles and then extrapolated towards q = 0). One notices a strong increase of w_{slow} which follows over a wide concentration range the power law

$$w_{slow} \sim (c/c^*)^{0.6} \quad (26)$$

Assuming a validity of this power law over an even wider concentration range the curve in Fig. 12 may be extrapolated to $w_{slow} = 1$, which in the present case is reached at c ≈ 10c*. Beyond this concentration the system is filled totally with clusters, i.e. only beyond this concentration a transient network will be found, which is the starting position for de Gennes theory of semi-dilute solutions. Before this concentration the system is still in a pre-gel state.

The strong interaction of the slow mode motion with the matrix of surrounding chains is demonstrated with Fig. 13 where D_{slow} is plotted against $\langle S^2\rangle_c$. In free diffusion one has $D \sim 1/\langle S^2\rangle^{1/2}$ behavior but in the semi-dilute region we now find (Ref.31)

$$D_{slow} \sim \langle S^2\rangle^{-(0.9\pm0.1)} \quad (27)$$

i.e. a much sharper reduction of the translational mobility.

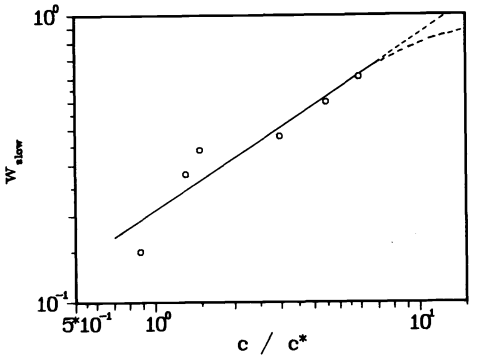

Fig. 12. Amplitudes w_{slow} of the slow mode as function of c/c*

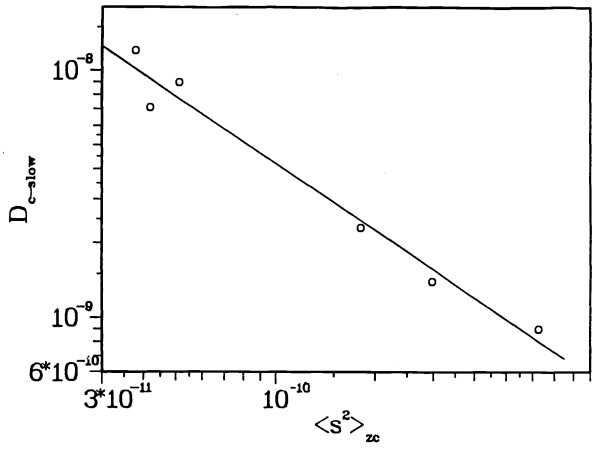

Fig. 13. Double logarithmic plot of D_{slow} against $\langle s^2 \rangle_c$.

We conclude this contribution with two further remarks concerning the two other diffusion coefficients plotted in Fig. 10.
(1) The cooperative or mutual diffusion coefficient D_{coop} is obtained from the first cumulant of the TCF when Γ/q^2 is extrapolated against q = 0. The result is shown in Fig. 10. Clearly D_{coop} agrees with D_{fast} only at low concentrations.
(2) According to irreversible thermodynamics the mutual diffusion coefficient is determined by a thermodynamic and a hydrodynamic friction contribution and is given by (Ref.19,33)

$$D_{coop} = (M_w/N_A f_c) \frac{\partial \pi}{\partial c} (1-cv_2) \qquad (28)$$

where f_c is the friction coefficient of the particles at concentration c. The osmotic compressibility $\partial\pi/\partial c$ can be obtained from the simutaneously recorded static LS which is given by

$$(Kc/R(q))_{q=0} = (RT)^{-1} (\partial\pi/\partial c) = 1/M_{app} \qquad (29)$$

Hence (Ref.31)

$$D_{coop} = (kT/f_c)(M_w/M_{app})(1-cv_2) \qquad (30)$$

The term kT/f_c D_{cm} corresponds to a diffusion coefficient, where the suffix 'cm' stands for center of mass. f_c corresponds to the frictional coefficient in a pre-gel state which is measured by sedimentation. D_{cm} contains still the contributions of the fast and the slow modes and cannot be considered as a self diffusion coefficient.

ACKNOWLEDGEMENT

We are indebted to many of our colleagues for valuable discussions, in particular to Dr. W. Brown, Uppsala Sweden, Dr. G.D. Patterson, Bell Laboratories and Dr. C. Cohen, Cornell University. This work was supported by the Deutsche Forschungsgemeinschaft.

REFERENCES

1. B. J. Berne and R. Pecora, "Dynamic Light Scattering", Wiley, New York (1976).
2. A. A. Michelson, Philos. Mag. 34, 280 (1892).
3. Ch. Fabry and H. Buisson, C.R. Acad.Sci. (Paris) 154,1224, 1500 (1912).
4. (a) G. Benedek, J.B. Lastovka ,K. Frisch, and T. Greytak, J.Opt.Soc.AM. 54, 1284 (1964).
   (b) S. B.. Dubin, J. H. Lunacek and G. Benedek Proc.Natl.Acad.Sci.US 57, 1164 (1967).
5. H. Z. Cummins, N. Knable and Y. Yeh, Phys.Rev.Letters 12, 150 (1964).
6. N. Wiener, Acta Math., 55, 117 (1930).
7. A. J. Khintchine, Math.Annalen 109, 604 (1934).
8. E. Jakeman, C. J. Oliver and E. R. Pike, J.Phys.A. 1, 406 (1968).
9. See Ref. 1.
10. R. Pecora in "Photon Correlation and Light Beating Spectroscopy", Plenum, New York (1973), p.387
11. D. E. Koppel, J.Chem.Phys 57, 4814 (1972).
12. P. Pusey, in "Photon Correlation Spectroscopy", Plenum, New York (1973), p. 387
13. Z. A. Akcasu and H. Gurol, J.Polymer Sci. Phys.Ed. 14, 1 (1976).
14. W. Burchard, M. Schmidt and W. H. Stockmayer, Macromolecules 13, 1265 (1980).
15. S. Bantle, M. Schmidt and W. Burchard, Macromolecules 15, 1604 (1982).
16. H. Yamakawa, J.Chem. Phys. 36, 2995 (1962).
17. C. W. Pyun and M. Fixman, J.Chem.Phys. 41, 937 (1964).
18. S. Imai, J.Chem.Phys. 50,2116 (1969).
19. H. Yamakawa, "Modern Theory of Polymer Solution", Harper & Row, New York (1971).
20. H.-U. ter Meer, W. Burchard and W. Wunderlich, Colloid & Polymer Sci., 258, 675 (1983).
21. K. Huber, Diploma Thesis, Freiburg (1983).
22. P.-G. de Gennes, "Scaling Concepts in Polymer Physics", Cornell University Press, Ithaca (1979).
23. T. Tanaka, L. Hocker and G. Benedek, J.Chem. Phys. 59, 5151 (1973).
24. P.-G.de Gennes, Nature 282, 367 (1979).
25. P. Mathiez, G. Weisbuch and C. Mouttet, Biopolymers 18, 1465 (1979).
26. (a) E. J. Amis, P. A. Janmey, J. D. Ferry and H. Yu, Macromolecules 16, 441(1983).
   (b) E. J. Amis and C. C. Han, Polymer 13,1403 (1982).
27. G. D. Patterson, personal communication
28. W. Brown, P. Stilbs and R. Johnson, J.Polymer Sci. Phys. Ed. 20 1771 (1980); personal communication.
29. J. C. Selzer, J.Phys.Chem. 79, 1044 (1983).
30. T. Nose and K. Tanaka,IUPAC Preprints, Amherst (1982) p. 715
31. M. Eisele and W. Burchard, Macromolecules submitted.
32. M. Daoud, Macromolecules 8, 804 (1974).
33. S. De Groot and P. Mazur, "Thermodynamics of Irreversible Processes", North Holland, Amsterdam (1952).
34. S. Candau, J. Bastide and M. Delsanti, Adv,Polymer Sci. 44, 27 (1982).
35. S. W. Provencher, Biophys.J. 16, 27 (1976).
36. D.-H. Hwang and C. Cohen, Macromolecules (1984) in print.